Fluids and Barriers of the CNS

RESEARCH

Open Access

Regulation of folate transport at the mouse arachnoid barrier

Vishal Sangha[1], Sara Aboulhassane[1] and Reina Bendayan[1*]

Abstract

Background Folates are a family of B_9 vitamins essential for normal growth and development in the central nervous system (CNS). Transport of folates is mediated by three major transport proteins: folate receptor alpha (FRα), proton-coupled folate transporter (PCFT), and reduced folate carrier (RFC). Brain folate uptake occurs at the choroid plexus (CP) epithelium through coordinated actions of FRα and PCFT, or directly into brain parenchyma at the vascular blood–brain barrier (BBB), mediated by RFC. Impaired folate transport can occur due to loss of function mutations in FRα or PCFT, resulting in suboptimal CSF folate levels. Our previous reports have demonstrated RFC upregulation by nuclear respiratory factor-1 (NRF-1) once activated by the natural compound pyrroloquinoline quinone (PQQ). More recently, we have identified folate transporter localization at the arachnoid barrier (AB). The purpose of the present study was to further characterize folate transporters localization and function in AB cells, as well as their regulation by NRF-1/PGC-1α signaling and folate deficiency.

Methods In immortalized mouse AB cells, polarized localization of RFC and PCFT was assessed by immunocytochemical analysis, with RFC and PCFT functionality examined with transport assays. The effects of PQQ treatment on changes in RFC functional expression were also investigated. Mouse AB cells grown in folate-deficient conditions were assessed for changes in gene expression of the folate transporters, and other key transporters and tight junction proteins.

Results Immunocytochemical analysis revealed apical localization of RFC at the mouse AB epithelium, with PCFT localized on the basolateral side and within intracellular compartments. PQQ led to significant increases in RFC functional expression, mediated by activation of the NRF-1/PGC-1α signalling cascade. Folate deficiency led to significant increases in expression of RFC, MRP3, P-gp, GLUT1 and the tight junction protein claudin-5.

Conclusion These results uncover the polarized expression of RFC and PCFT at the AB, with induction of RFC functional expression by activation of the NRF-1/PGC-1α signalling pathway and folate deficiency. These results suggest that the AB may contribute to the flow of folates into the CSF, representing an additional pathway when folate transport at the CP is impaired.

Keywords Folates, Arachnoid barrier, Reduced folate carrier, Proton-coupled folate transporter, Folate receptor, Pyrroloquinoline quinone, Blood-cerebrospinal fluid barrier

Introduction

Folates are a family of B_9 vitamins that are essential for normal growth and development in the central nervous system (CNS), with folate deficiency serving as a risk factor for neural tube defects (NTDs), cardiovascular disorders and cancer [1, 2]. In mammals, folates are transported by three processes: (i) the high affinity folate

*Correspondence:
Reina Bendayan
r.bendayan@utoronto.ca
[1] Leslie Dan Faculty of Pharmacy, University of Toronto, Toronto, Canada

receptors (gene: *FOLR1-2/Folr1-2*), functioning through receptor-mediated endocytosis [3], (ii) the reduced folate carrier (RFC) (gene: *SLC19A1/Slc19a1*), an organic phosphate antiporter which optimally operates at pH 7.4. [4, 5], and (iii) the proton-coupled folate transporter (gene: *SLC46A1/Slc46a1*), a proton co-transporter displaying optimal activity at pH 4.5–5.5 [6, 7].

The major routes of CNS folate uptake include the choroid plexus (CP) epithelium of the blood-cerebrospinal fluid barrier (BCSFB) and the vascular blood–brain barrier (BBB) [8–11]. FRα represents a major transcytosis pathway for folates at the BCSFB, with PCFT assisting in this transport [8, 12]. Impairments in FRα function can result in *FOLR1*-related cerebral folate transport deficiency (*FOLR1*-CFTD) [13–15]. The presence of folate receptor autoantibodies (FRAAs) impairing FRα function can also result in brain folate deficiency, and has been recognized in neurological disorders including autism spectrum disorder (ASD) [16]. Impaired PCFT function is the basis for hereditary folate malabsorption (HFM) resulting in both cerebral and systemic folate deficiency [6, 17].

Our previous reports have demonstrated the importance of the BBB in cerebral folate delivery, as functional upregulation of RFC at this barrier results in enhanced brain folate uptake in the context of FRα impairment at the CP [9–11]. In mice lacking FRα, induction of RFC function by the vitamin D receptor (VDR) effectively restored brain folate levels, representing a potential novel therapeutic strategy for *FOLR1*-CFTD [10]. Additionally, nuclear respiratory factor 1 (NRF-1), a transcription factor involved in regulating mitochondrial function was shown to induce RFC expression and function in models of the BBB and brain parenchyma [11, 18]. NRF-1 can be indirectly activated by the naturally derived enzyme cofactor pyrroloquinoline quinone (PQQ) through peroxisome proliferator-activated receptor-γ coactivator-1α (PGC-1α) [19, 20]. We have also shown that PQQ can exert anti-inflammatory, antioxidant, and mitochondrial biogenesis effects in brain folate deficiency. PQQ may assist in enhancing folate transport, while in parallel alleviating the physiological impairments of brain folate deficiency. [18]

The arachnoid barrier (AB) represents an additional interface between the CSF and peripheral circulation that may be involved in regulating CSF homeostasis [21, 22, 27]. This barrier is at the interface of the dura and pia mater and regulates the exchange between the dural vasculature and CSF [21–24, 27]. The subarachnoid space contains about 80% of the total CSF volume in the brain compared to the ventricles [25]. Several members of the ATP-binding cassette (ABC) and solute carrier (SLC) superfamilies are highly expressed at the AB and may play a significant role in CSF regulation (Fig. 1) [21, 26].

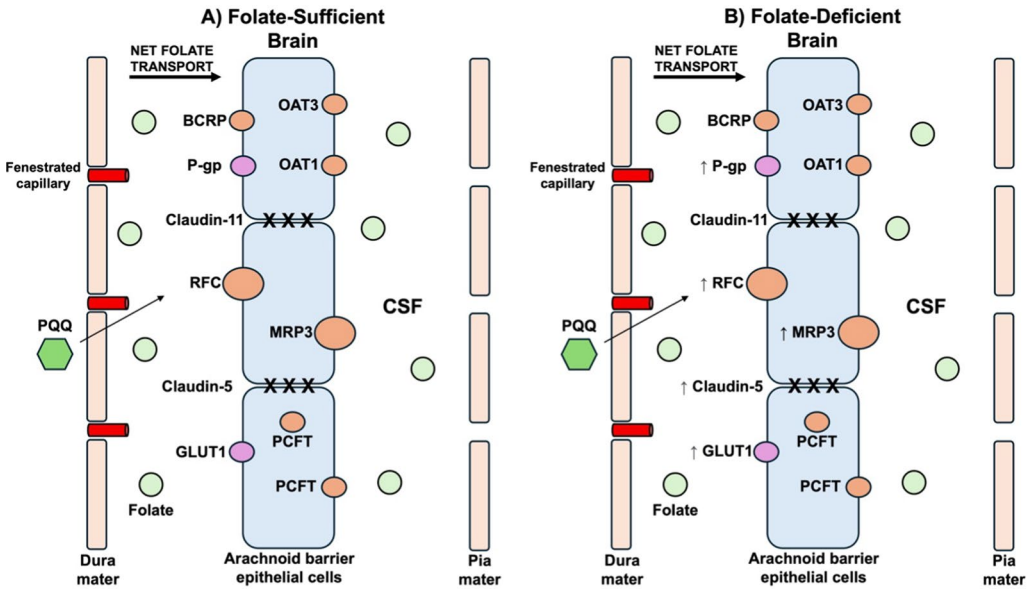

Fig. 1 Proposed mechanism of folate transport at the arachnoid barrier (AB). **A** Folates are transported from the dural vasculature into AB epithelial cells by RFC, which is localized on the apical membrane. Folates are further shuttled into the subarachnoid space containing CSF through MRP3, which is localized on the basolateral membrane. PCFT is localized on the basolateral membrane and within intracellular compartments of the AB, but likely does not contribute to this transport due to its optimal activity conditions at acidic pH. **B** Folate deficiency results in AB dysregulation, with increased expression of RFC, MRP3, P-gp, and GLUT1. Dysregulation of the tight junction proteins are also observed through upregulation of claudin-5. In both folate-sufficient and FD conditions, PQQ results in RFC upregulation (figure adapted from [21])

We have reported localization and expression of RFC and PCFT at the AB, while FRα is absent [27]. The goal of the present study was to further characterize the localization and functional expression of folate transporters in AB cells, as well as their regulation by NRF-1/PGC-1α and folate deficiency. This work provides novel insight on the role of the AB cells in cellular folate uptake, particularly under conditions in which FRα-mediated transport at the CP is impaired.

Materials and methods

Materials

All cell culture reagents used for in vitro experiments were purchased from Invitrogen (Carlsbad, CA, USA) unless indicated otherwise. PQQ was purchased from Cayman Chemicals (Ann Arbor, MI, USA). For immunocytochemistry analysis, primary rabbit polyclonal anti-RFC antibody (MBS9134642) was purchased from MyBioSource (San Diego, CA, USA). Rabbit polyclonal anti-PCFT antibody (ab25134) was purchased from Abcam Biotechnology (Cambridge, MA, USA). Primary mouse monoclonal anti-Na^+/K^+-ATPase α antibody (sc-58628) was obtained from Santa Cruz Biotechnology (Dallas, TX, USA). For transport assays, tritium labelled [^{3}H]-methotrexate (MTX) and [^{3}H]-folic acid (FA) were obtained from Moravek Biochemicals (Brea, CA, USA). Unlabelled methotrexate, folic acid and pemetrexed were obtained from Sigma-Aldrich (Oakville, ON, Canada). Real time quantitative polymerase chain reaction (qPCR) reagents, including reverse transcription cDNA kits were purchased from Applied Biosystems (Foster City, CA, USA). qPCR primers were purchased from Life Technology and were validated for use with TaqMan qPCR chemistry (Carlsbad, CA, USA). For western blot experiments, primary rabbit polyclonal anti-SLC19A1 (AV44167), and primary rabbit polyclonal anti-SLC46A1 (PCFT) antibody (SAB2108339) were purchased from Sigma-Aldrich. Mouse monoclonal anti-β-actin antibody (sc-517582) was obtained from Santa Cruz Biotechnology. Anti-rabbit Alexa Fluor 594 and anti-mouse Alexa Fluor 488–conjugated secondary antibodies were purchased from Invitrogen.

Cell culture

Immortalized mouse AB cells were kindly provided by Dr. Erin Schuetz (St. Jude's Children's Research Hospital, Memphis, TN, USA). AB cells (passage 3–10) were cultured in DMEM supplemented with 9% FBS, 1% horse serum, 1×penicillin/streptomycin, 1×fungizone, and 1×glutamine and grown on 75 cm^2 poly-D-lysine (PDL) coated flasks as previously described [22, 27, 28]. Cells were maintained in a humidified incubator at 37°C, 5% CO_2, and 95% of air atmosphere, with fresh media replaced every 72 h. For studies examining the effects of folate deficiency, cells were grown in a custom Dulbecco's modified Eagle medium (DMEM) lacking folic acid as previously used in our laboratory. We confirmed folate deficiency through quantification of folate levels applying the microbiological assay [18]. Upon reaching confluence, cells were collected and further processed for downstream analysis.

Immunocytochemical analysis

Polarized localization of the folate transport systems (RFC, PCFT) was examined in immortalized mouse AB cells grown to confluence on 3.0-μm polyester transwell inserts in 12-well plates (Corning Inc, NY, USA). Cells were fixed with 4% PFA for 20 min, followed by permeabilization with 0.1% Triton X-100. Following permeabilization, inserts were carefully removed from the wells for further processing. Further immunocytochemical analysis was performed as described in Sangha et al. [27]. Primary rabbit polyclonal anti-RFC (1:100) and anti-PCFT (1:50) antibodies were used to detect RFC and PCFT, respectively. To visualize the cell membrane, cells were stained with mouse monoclonal anti-Na^+/K^+-ATPase α (sc-58628) (1:50), with anti-rabbit Alexa Flour or anti-mouse Alexa Flour 488-conjugated used as secondary antibodies (1:500). As a negative control, cells were incubated with only secondary antibody to confirm primary antibody specificity. Cell staining was visualized using an LSM 700 laser-scanning confocal microscope (Carl Zeiss AG) at a 63×objective lens operated with ZEN Software. Z-stack images were obtained using the ZEN software and *xz* and *yz* images were acquired to visualize the apical and basolateral membrane localization of the folate transporters.

Transport assays

To assess the functional activity of RFC and PCFT in immortalized AB cells, transport assays were conducted in AB cells grown until confluence in 24-well plates with 50 nM [^{3}H]-MTX (an RFC substrate) or 50 nM [^{3}H]-FA (a PCFT substrate) following standard procedures in our laboratory as previously described [9, 29]. All transport assays were performed using transport buffer [Hank's balanced salt solution supplemented with 0.01% BSA and 25 mM HEPES (pH 7·4) or 25 mM MES (pH 5.5)], with initial uptake rates assessed by examining cellular uptake of [^{3}H]-MTX or [^{3}H]-FA at several time points (0 s–30 min). Transport assays assessing RFC function were performed at extracellular pH 7.4 and assays assessing PCFT function were performed at extracellular pH 5.5 which reflect optimal activity conditions for both transporters [9, 29]. To examine the specificity of transport activity, RFC/PCFT inhibitor pemetrexed (10 μM)

and excess unlabelled substrate (10 μM) were added to both pre-incubation and transport buffers. For all transport experiments, 10 μM elacridar (GF120918) was added to preincubation and transport buffers to prevent any possible contribution of P-gp or BCRP in substrate uptake [30]. To correct for non-specific binding and variable quench time, cellular uptake of the radiolabelled substrate was determined after zero time of exposure. Cellular uptake of radiolabelled FA or MTX was normalized to total protein content per well, quantified by the Bio-Rad DC Protein Assay kit with BSA as a standard (Bio-rad Laboratories, Hercules, CA, USA).

PQQ treatments

For gene and protein expression studies, confluent mouse AB cells grown in 25 cm^2 flasks were treated with PQQ (1, 5, 10 μM) or dimethyl sulfoxide (DMSO) vehicle for 24 or 48 h at 37 °C. Following the desired time interval, cells were collected and processed for qPCR and western blot analysis. For transport studies, confluent mouse AB cells grown in 24-well plates were treated with 10 μM PQQ or DMSO vehicle for 24 h at 37 °C. Studies examining changes in gene expression in folate-deficient (FD) AB cells were performed with 5 μM and 10 μM PQQ at 24h, as these doses and time point yielded the most robust results in our control data. To confirm that there were no toxicities observed at the desired PQQ concentrations, an MTT assay was perform in control and FD cells to observe potential changes in cell viability (Additional file 1: Fig. S1).

Gene expression analysis

Changes in mRNA expression of the various genes of interest was assessed in mouse AB cells using qPCR analysis as previously described in our laboratory [18]. Mouse primers for the following genes were obtained from Life Technologies for use with Taqman qPCR chemistry: *Slc19a1* (RFC; Mm00446220_m1), *Slc46a1* (PCFT; Mm00546630_m1), *Nrf1* (NRF-1; Mm01135606_m1), *PPargc1a* (PGC-1α; Mm01208835_m1), *Tfam* (Tfam;Mm00447485_m1), *Tfb1m* (TFB1M; Mm00524825_m1), *Tfb2m* (TFB2M; Mm01620397_s1), *Abc1b* (P-gp; Mm00440736_m1), *Abcg2* (Bcrp; Mm00496364_m1), *Abcc3* (Mrp3; Mm00551550_m1), *Cldn5* (Claudin-5; Mm00727012_s1), *Cldn11* (Claudin-11; Mm00500915_m1), *Slc22a6* (OAT1; Mm00456258_m1), *Slc22a8* (OAT2; Mm00459534_m1), *Slc1a3* (GLUT1; Mm00600697_m1). For all gene expression assays, experiments were performed in triplicates using the housekeeping gene mouse cyclophilin B as an internal control. For each gene assessed, relative mRNA expression was measured by calculating the difference in CT values (ΔCT) between the target gene and cyclophilin B.

Protein expression analysis

Western blot analysis was performed according to standard procedures in our laboratory and as described in Sangha et al. [27]. Protein bands of interest were examined using primary rabbit polyclonal anti-SLC19A1 (RFC) antibody (1:250), rabbit polyclonal anti-SLC46A1 (PCFT) antibody (1:250) or mouse monoclonal anti-β-actin antibody (1:1000). Horseradish peroxidase-conjugated anti-rabbit (1:5000) or anti-mouse (1:5000) was used as a secondary antibody. Protein bands of interest were detected using enhanced chemiluminescence SuperSignal West Pico System (Thermo Fisher Scientific) and images were taken using the ChemiDoc MP Imaging System (Bio-Rad). For all experiments, 50 μg of protein was loaded per well, with expression quantified relative to β-actin by densitometric analysis.

Statistical analysis

All statistical analysis was performed using Prism 10 software (GraphPad Software Inc., San Diego, CA, United States). For all in vitro work, experiments were repeated at least three times using separate mouse AB cell preparations. Results are presented as mean ± SEM. Multiple group comparisons were performed using one-way analysis of variance (ANOVA) with Bonferroni's post hoc test. For all statistical tests performed, $P < 0.05$ was considered statistically significant.

Results

Polarized membrane localization of RFC and PCFT in mouse AB cells

The polarized membrane localization of RFC and PCFT was examined through immunocytochemical analysis. As the AB layer shows a continuous basal lamina on its inner surface facing the CSF, the surface of the AB cell facing the CSF is the basolateral side [24, 28, 31]. Conversely, the cell layer facing the dura (or the blood side) is the apical membrane [28]. Immunocytochemical analysis revealed robust RFC staining on the apical membrane of the mouse AB cells in comparison to the basolateral membrane (Fig. 2A). In contrast, prominent PCFT staining is detected on the basolateral membrane in comparison to the apical membrane of mouse AB cells. Additionally, PCFT staining is observed in intracellular compartments of the mouse AB cells (Fig. 2B).

Effects of PQQ treatment on folate transporter expression in mouse AB cells

PGC-1α mRNA expression was increased by ~ 50% ($P = 0.002$) and ~ 80% ($P < 0.0001$) in AB cells following

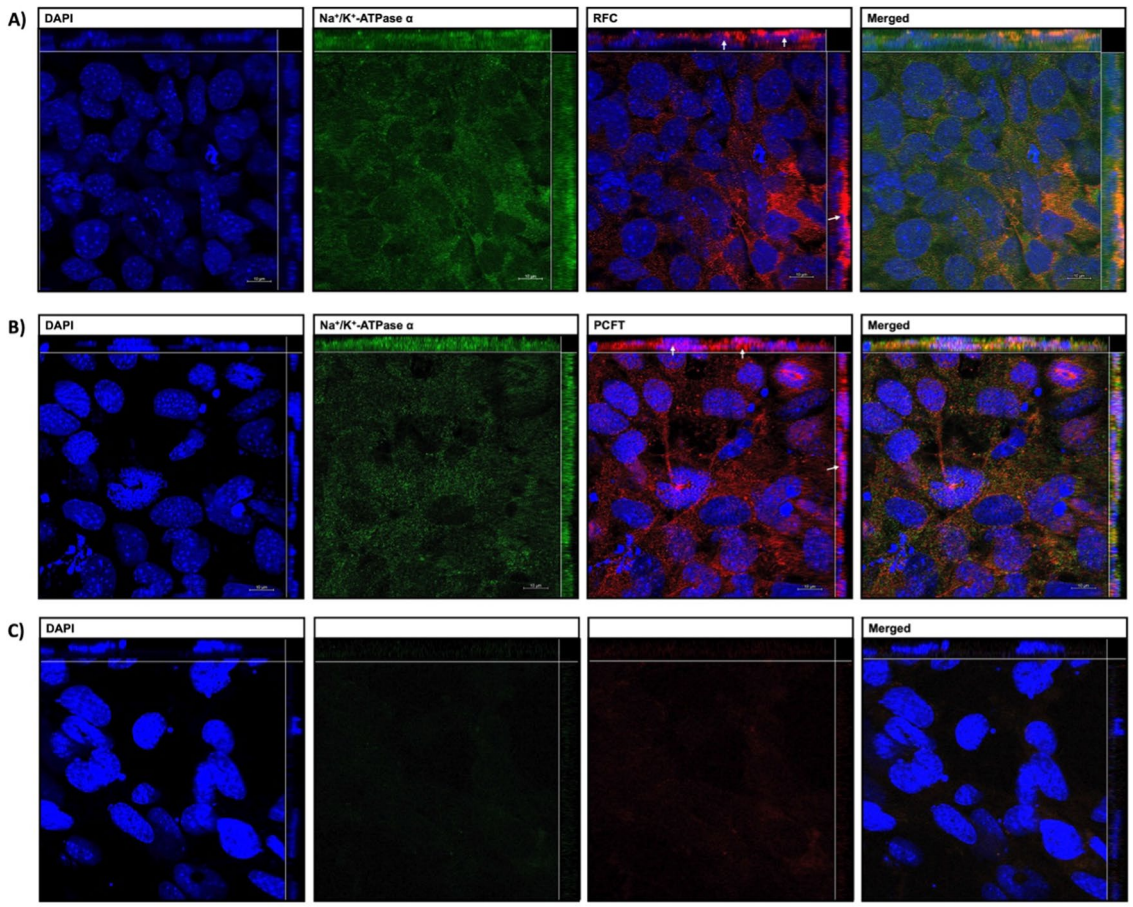

Fig. 2 Polarized localization of RFC and PCFT in immortalized mouse AB cells. Cells grown until confluence on transwell permeable support were fixed and stained with the following: DAPI nuclear marker, anti-RFC (1:100) (**A**) or anti-PCFT (1:50) (**B**). To visualize the cell membrane, AB cells were stained with the membrane marker Na^+/K^+-ATPase α (1:50). No primary antibody was used as a negative control (**C**). Arrows denote polarized localization of RFC/PCFT. Cells were visualized using confocal microscopy (LSM 700; Carl Zeiss) operated with ZEN software using an oil-immersion 63 × lens. *xy* and *xz* sections were further obtained with ZEN software

exposure to 1 μM and 10 μM PQQ for 24-h, respectively (Fig. 3A). No changes in NRF-1 expression were observed in response to PQQ [11, 18]. Tfam and TFB2M expression was increased by ~ 55% (P = 0.003) and ~ 60% (P = 0.01) following 24-h 5 μM PQQ, respectively (Fig. 3B, C). TFB1M expression was increased by ~ 75% (P = < 0.0001) following 5 μM PQQ for 48-h (Additional file 1: Fig. S2D). RFC expression was increased by ~ 45% (P = 0.0002) and ~ 60% (P < 0.0001) following 5 μM and 10 μM PQQ for 24-h, respectively (Fig. 4A). RFC protein expression was increased by ~ 50% (P = 0.003) at 65 kDa following 10 μM PQQ, while both 5 μM and 10 μM PQQ increased RFC expression by ~ 50% (P = 0.02) and ~ 80% (P = 0.0005) at 63 kDa, respectively (Fig. 4B). No changes in PCFT mRNA or protein expression were detected in AB cells in response to PQQ (Additional file 1: Fig. S3).

Functional activity of RFC and PCFT in mouse AB cells

To assess RFC function, [^{3}H]-MTX (50 nM) uptake was measured over 30 min, with a linear uptake observed up to 1 min (net influx) (Fig. 5A). In the presence of pemetrexed (10 μM) and excess unlabelled MTX (10 μM), [^{3}H]-MTX uptake was decreased by ~ 40% (P = 0.04) and ~ 50% (P = 0.01) at 30 s, and ~ 60% (P = 0.0002) and ~ 40% (P = 0.005) at 60 s, respectively (Additional file 1: Fig. S4). [^{3}H]-MTX uptake was increased by ~ 40% following 10 uM PQQ treatment at 30 s (P = 0.04) and 60 s (P = 0.005) (Fig. 5B). In the presence of pemetrexed (10 μM), the effects of PQQ were abolished, reducing [^{3}H]-MTX uptake by ~ 30% (P = 0.0009) and ~ 35% (P = < 0.0001) at 30 and 60 s, respectively (Fig. 5C). To assess PCFT function, [^{3}H]-FA (50 nM) uptake was measured over 30 min, with a linear uptake observed up to 1 min (net influx) (Additional file 1: Fig. S5). In the presence of pemetrexed (10 μM) and excess unlabelled

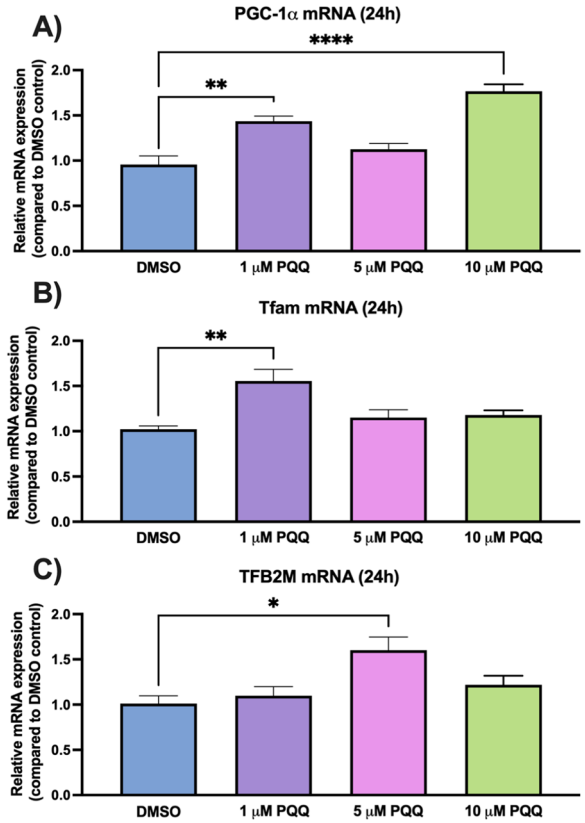

Fig. 3 Effect of PQQ on expression of PGC-1α signaling genes in immortalized mouse AB cells. **A** PGC-1α expression was significantly increased in mouse AB cells following 24-h PQQ (1 μM, 10 μM. **B** Tfam expression was significantly increased in AB cells following 24-h (1 μM) PQQ. **C** TFB2M expression was significantly increased in AB cells following 24-h PQQ (5 μM). Results are presented as mean relative mRNA expression compared to the DMSO vehicle control ± SEM normalized to the housekeeping gene cyclophilin B from n = 5 mouse AB cell preparations pertaining to different passages. One-way ANOVA with Bonferroni's post-hoc test. Asterisks represent significant differences (*P < 0.05; **P < 0.01; ****P < 0.0001)

MTX (10 μM), [^{3}H]-FA uptake was decreased by ~ 70% (P = 0.01) and ~ 50% (P = 0.009) at 30 s, and ~ 65% (P = 0.04) and ~ 45% (P = 0.03) at 60 s, respectively (Additional file 1: Fig. S5).

Effects of folate deficiency and PQQ treatment on NRF-1/PGC-1α signaling and folate transporters in mouse AB cells

No alterations in PGC-1α mRNA expression were observed in FD cells. Exposure to 10 μM PQQ increased PGC-1α expression by ~ 50% in control folate-sufficient (P = 0.02) and FD cells (P = 0.02) (Fig. 6A). NRF-1 expression was increased by ~ 30% in FD cells (P = 0.05) (Fig. 6B). In contrast, PQQ did not affect NRF-1 expression in either control or FD cells (Fig. 6B). Tfam expression was increased by ~ 30% in FD cells (P = 0.03) (Fig. 6C) while PQQ did not affect Tfam or TFB1M expression (Fig. 6C). TFB2M expression was increased by ~ 70% in FD cells (P = 0.007) and increased by ~ 100% (P = 0.003) and ~ 60% (P = 0.04) in control cells following 5 μM and 10 μM PQQ, respectively (Fig. 6D). RFC expression was increased by ~ 35% (P = 0.04) in FD cells, with an increase of ~ 45% (P = 0.005) and ~ 50% (P = 0.001) in control cells following 5 μM and 10 μM PQQ, respectively (Fig. 7). In FD cells, 10 μM PQQ led to an ~ 25% increase (P = 0.02) in RFC expression (Fig. 7A). PCFT expression remained unchanged in FD conditions and after PQQ.

Effects of folate deficiency and PQQ treatment on the expression of additional key ABC/SLC transporters and tight junction proteins in mouse AB cells

Changes in mRNA expression of additional ABC/SLC transporters localized at the AB were also assessed in FD conditions [21, 32]. MRP3 expression was increased in FD cells by ~ 100% (P = 0.002) (Fig. 7B) and P-gp and GLUT-1 expression were increased by ~ 50% in FD cells (P-gp: P = 0.0004; GLUT-1: P = 0.003) (Fig. 7C). There were no changes in expression of BCRP, OAT1, and OAT3 in FD cells (Additional file 1: Fig. S6). MRP4 expression was undetected in this AB cell culture system. PQQ treatment did not affect the expression of the other ABC/SLC transporters (i.e., MRP3, BCRP, OAT1, OAT3, P-gp, GLUT1) in control or FD cells (Fig. 7B–D, Additional file 1: Fig. S6). PQQ (5 μM) led to an increase of ~ 35% (P = 0.02) in claudin-5 expression in control cells, and ~ 40% (P = 0.004) in FD cells (Fig. 8). No changes in claudin-11 expression were observed in FD cells and in response to PQQ (Additional file 1: Fig. S6).

Discussion

Folates are transported from the peripheral circulation into the CSF at the BCSFB and into brain parenchymal cells at the vascular BBB to meet the substantial metabolic demands of the CNS [8–11]. Impairment in folate transport can result in pediatric neurological disorders including *FOLR1*-CFTD and HFM [13, 15, 17]. Our previous studies have reported upregulation of RFC at the BBB by the transcription factors VDR and NRF-1 and suggested that this may be a novel treatment strategy for brain folate deficiency disorders that affect the CP [9–11].

In the current study, immunocytochemical analysis demonstrated preferential apical localization of RFC in AB cells suggesting that RFC may shuttle folates from the dural vasculature into the AB epithelium. RFC plays a similar role at the BBB, localized on the luminal membrane of the brain microvessel endothelium, facilitating folate uptake into the brain parenchyma [10, 33]. PCFT staining was observed on the basolateral side and

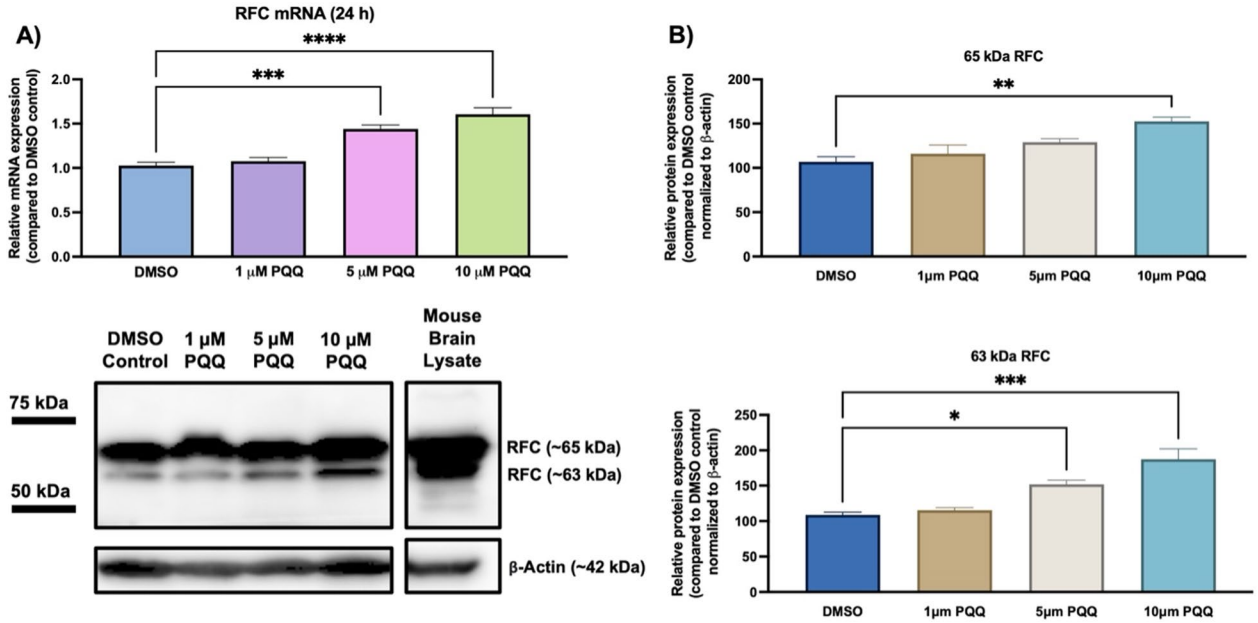

Fig. 4 Effect of PQQ on RFC gene and protein expression in immortalized mouse AB cells. **A** RFC gene expression was significantly increased in mouse AB cells following 24-h PQQ (5 μm, 10 μm). **B** Significant increases in RFC protein expression were observed in mouse AB cells following 24-h PQQ (5 μM, 10 μM) compared to DMSO control. Multiple protein bands for RFC (63, 65 kDa) are indicative of differential glycosylation of the transmembrane protein. Mouse brain lysates served as positive control, while actin was used as a loading control. mRNA expression data is presented as mean relative mRNA expression compared to the DMSO vehicle control ± SEM normalized to the housekeeping gene cyclophilin B from n = 5 mouse AB cell preparations pertaining to different passages. Protein expression data is presented as mean ± SEM from n = 3 mouse AB cell preparations pertaining to different passages. One-way ANOVA with Bonferroni's post-hoc test. Asterisks represent significant differences (*P < 0.05; **P < 0.01; ***P < 0.001; ****P < 0.0001)

within intracellular compartments, which may represent membrane-associated PCFT in vesicles involved in transepithelial transport, even in the absence of FRα. RFC and PCFT were both expressed and functional in AB cell monolayers suggesting that one or both have a role in mediating folate uptake at the AB. While PCFT may not play a significant role in cerebral folate uptake at the AB, it may serve as a clinically relevant transporter in the context of antifolate delivery in the acidic microenvironment of meningeal neoplasms [34].

We have previously reported that activation of NRF-1/PGC-1α signaling by PQQ, with the direct involvement of NRF-1, induces RFC expression. This was confirmed by a chromatin immunoprecipitation (ChIP) assay and siRNA knockdown studies [11, 18]. In the present study, PQQ increased PGC-1α and downstream NRF-1 target expression, accompanied by increases in RFC expression in AB cells, as previously demonstrated in vitro and in vivo [11, 18]. No changes in PCFT expression were observed in response to PQQ, which contrasts with our previous studies reporting PQQ-mediated increases in PCFT expression in primary cultures of mouse mixed glial cells and mouse brain tissue [18]. PQQ also enhanced RFC function at the AB. Taken together, RFC upregulation by NRF-1/PGC-1α at the BBB, AB, and brain parenchyma may work in concert to enhance brain folate uptake under conditions in which folate transport into the CSF is impaired as in HFM and *FOLR1*-CFTD.

Our previous reports showed that brain folate deficiency results in inflammation, mitochondrial dysfunction, and oxidative stress in vitro and in vivo. This is reversed by PQQ which also enhances folate transporter expression [18]. Folate deficiency disrupts tight junction proteins at the BBB [35]. BBB/BCSFB dysfunction has also been observed in inflammation and oxidative stress, altering expression of several transporters and tight junction proteins [36, 37]. In the current study, PQQ induced PGC-1α signaling resulting in increased expression of NRF-1 and TFB2M in FD cells. Similarly, PGC-1α, NRF-1 and Tfam were upregulated in folate deprived rats, possibly due to increases in mitochondrial biogenesis to compensate for reductions in mtDNA content in FD conditions [18, 38]. Similar to the increase in RFC expression in FD AB cells, RFC expression was increased in FD Caco-2 cells through activation of specificity protein 1 (Sp1), suggesting that

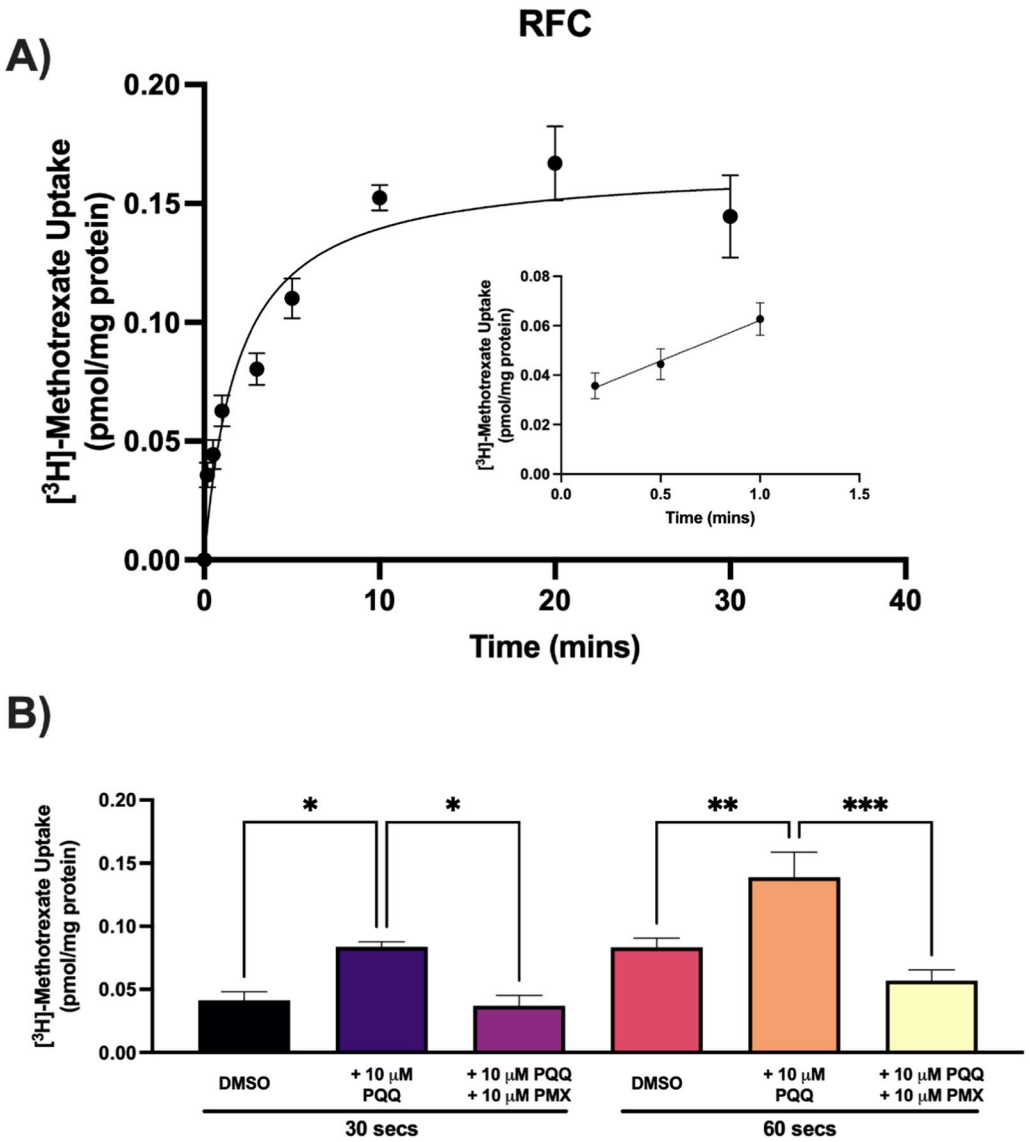

Fig. 5 Methotrexate uptake by immortalized mouse AB cells. **A** Time profile of [^{3}H]-methotrexate in immortalized mouse AB cells. The uptake of 50 nM [^{3}H]-methotrexate by the mouse AB monolayer was measured over 30 min at pH 7.4 and 37 °C. The inset shows the linearity of initial uptake up to 1 min. **B** Significant increases in cellular uptake of [^{3}H]-methotrexate was observed in mouse AB cells following 24-h PQQ (10 μM), at 30 and 60 s. PQQ-mediated increases in [^{3}H]-methotrexate uptake was inhibited by pemetrexed (10 μM). Results are presented as mean ± SEM from n = 4 mouse AB cell preparations pertaining to different passages. One-way ANOVA with Bonferroni's post-hoc test. Asterisks represent significant differences (*P < 0.05; **P < 0.01; ***P < 0.001)

NRF-1 may signal through additional regulatory pathways to induce RFC expression [39]. In both control and FD conditions, PQQ significantly increased RFC expression in AB cells indicating that PQQ signaling is present in both folate-sufficient and -deficient conditions. No changes in PCFT expression were observed in FD AB cells, which contrasts with previous data in mixed glial cells and reports of PCFT overexpression in FD conditions [39, 40] consistent with the observation that folate transporter expression in FD conditions may vary in different brain cellular compartments [18].

In the current study, MRP3, P-gp and GLUT1 expression was increased in in FD cells. MRP3 is localized on the basolateral membrane of these cells and may assist in the export of folates into the CSF; it has a similar location and plays a similar role in the intestinal absorption

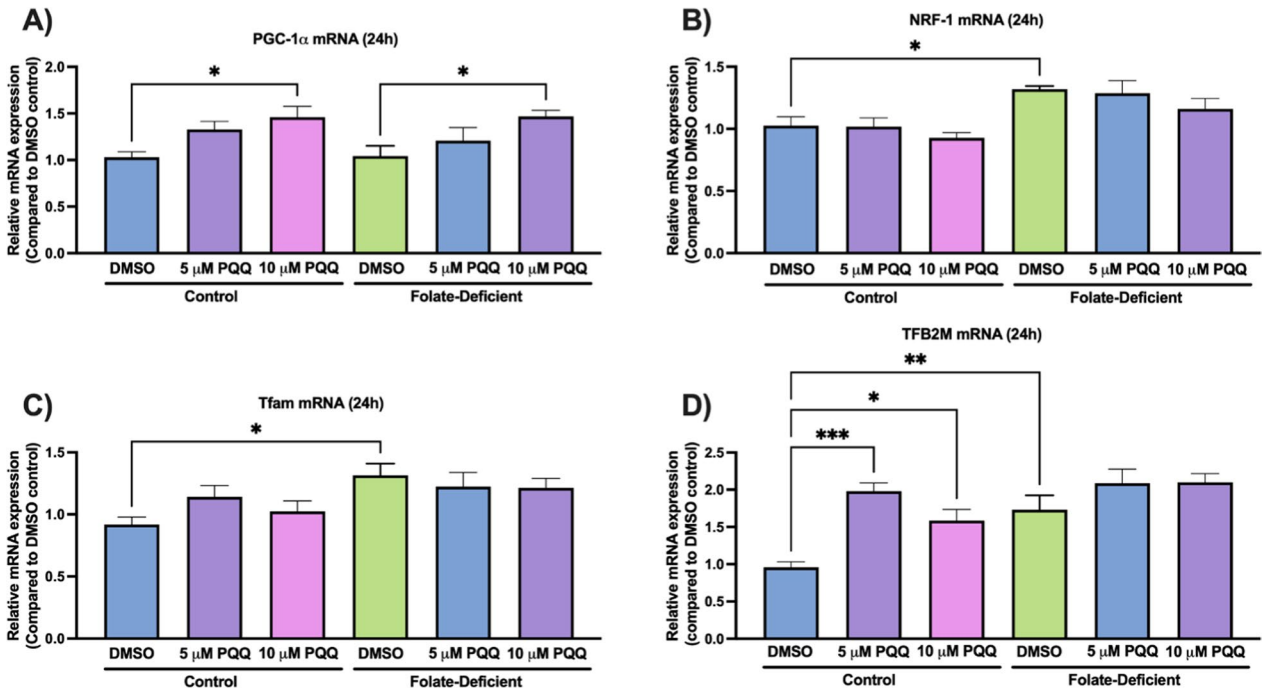

Fig. 6 Effect of folate deficiency and PQQ on gene expression of PGC-1α /NRF-1 signaling genes in immortalized mouse AB cells. **A** PGC-1α expression was significantly increased in control and FD cells following 24-h PQQ (10 μM). **B** NRF-1 expression was significantly increased in FD cells compared to control and remained unchanged in control and FD cells in response to 24-h PQQ. **C** Tfam expression was significantly increased in FD cells compared to control and remained unchanged in control and FD cells in response to 24-h PQQ. **D** TFB2M expression was significantly increased in FD cells compared to control and increased in control and FD cells in response to 24-h PQQ (5 μM, 10 μM). Results are presented as mean relative mRNA expression compared to the DMSO vehicle control ± SEM normalized to the housekeeping gene cyclophilin B from n = 5 mouse AB cell preparations pertaining to different passages. One-way ANOVA with Bonferroni's post-hoc test. Asterisks represent significant differences (*P < 0.05; **P < 0.01; ***P < 0.001)

of folates [21, 41, 42]. In FD conditions, increased RFC and MRP3 expression may compensate to restore brain folate levels. Changes in P-gp and GLUT1 expression in response to folate deficiency have not been reported previously, however these changes may be mediated by activation of nuclear factor kappa B (NF-κB), which in turn may upregulate these transporters [43–45]. Interestingly, PQQ failed to restore the expression of these transporters to baseline levels. Finally, folate deficiency increased expression of the tight junction protein, claudin-5, which may be related to the increase in RFC since increased RFC expression was reported to increase occludin and claudin-5 expression in the mouse inner blood-retinal barrier [46]. PQQ also led to increases in claudin-5 expression as also reported in intestinal porcine enterocyte cells (IPEC-J2) [47].

Conclusion

The present studies characterized the localization of folate transporters at the AB, uncovering a potential novel route of cerebral folate transport from blood to CSF. In the context of *FOLR1*-CFTD and HFM, RFC upregulation at the the AB and BBB may compensate for the loss of folate transport into the CSF at the CP. These studies also demonstrated folate deficiency-induced increases in expression of several clinically relevant transporters and tight junction proteins in AB cells and demonstrated the role of PQQ induced NRF-1/ PGC-1α signaling in folate-sufficient and -deficient conditions. Overall, this work extends the understanding of the regulation of folate transport within the CNS to encompass the AB and its role under physiological conditions and when transport at the CP is impaired.

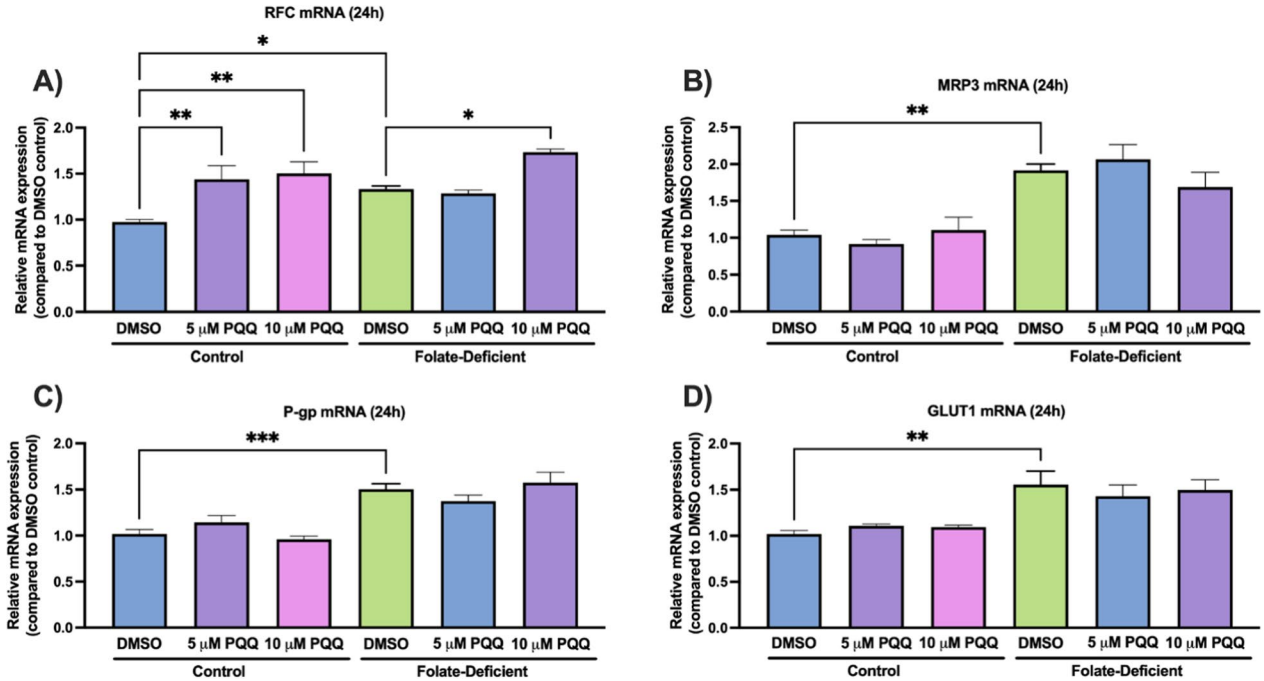

Fig. 7 Effect of folate deficiency and PQQ on transporters involved in folate influx/efflux in immortalized mouse AB cells. **A** RFC expression was significantly increased in FD cells compared to control, and significantly increased in control (5 µm, 10 µm) and FD cells (10 µm) following 24-h PQQ. **B** MRP3 expression was significantly increased in FD cells compared to control and remained unchanged in control and FD cells in response to 24-h PQQ. **C** P-gp expression was significantly increased in FD cells compared to control and remained unchanged in control and FD cells in response to 24-h PQQ. **D** GLUT1 expression was significantly increased in FD cells compared to control and remained unchanged in control and FD cells in response to 24-h PQQ. Results are presented as mean relative mRNA expression compared to the DMSO vehicle control ± SEM normalized to the housekeeping gene cyclophilin B from n = 5 mouse AB cell preparations pertaining to different passages. One-way ANOVA with Bonferroni's post-hoc test. Asterisks represent significant differences (*P < 0.05; **P < 0.01; ***P < 0.001)

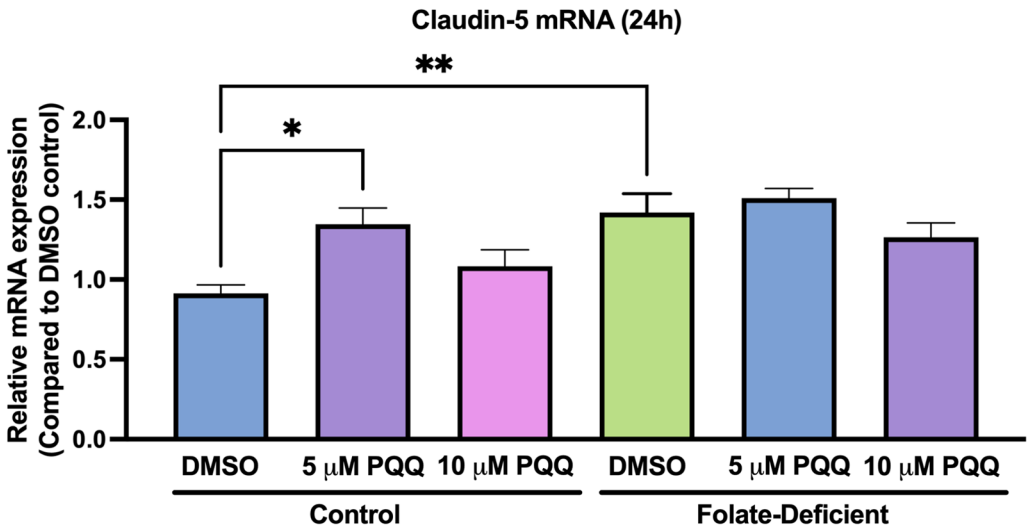

Fig. 8 Effect of folate deficiency and PQQ on gene expression of tight junction proteins in immortalized mouse AB cells. Claudin-5 expression was significantly increased in FD cells compared to control, and significantly increased in control cells following 24-h PQQ (5 µM). Results are presented as mean relative mRNA expression compared to the DMSO vehicle control ± SEM normalized to the housekeeping gene cyclophilin B from n = 5 mouse AB cell preparations pertaining to different passages. One-way ANOVA with Bonferroni's post-hoc test. Asterisks represent significant differences (*P < 0.05; *P < 0.01)

Abbreviations

AB	Arachnoid barrier
ABC	ATP-binding cassette
ANOVA	Analysis of variance
ASD	Autism spectrum disorder
BBB	Blood–brain barrier
BCRP	Breast cancer resistance protein
BCSFB	Blood-cerebrospinal fluid barrier
FOLR1-CFTD	*FOLR1*-Related cerebral folate transport deficiency
CNS	Central nervous system
CP	Choroid plexus
CSF	Cerebrospinal fluid
DMEM	Dulbecco's modified Eagle medium
DMSO	Dimethyl sulfoxide
FA	Folic acid
FD	Folate deficient
FRAA	Folate receptor autoantibodies
FRα	Folate receptor alpha
GLUT	Glucose transporter
MRP	Multidrug resistance protein
MTX	Methotrexate
NF-κB	Nuclear factor kappa B
NRF-1	Nuclear respiratory factor-1
NTDs	Neural tube defects
OAT	Organic anion transporter
P-gp	P-glycoprotein
PCFT	Proton-coupled folate transporter
PDL	Poly-D-lysine
PGC-1α	Peroxisome proliferator-activated receptor-γ coactivator-1α
PQQ	Pyrroloquinoline quinone
qPCR	Quantitative polymerase chain reaction
RFC	Reduced folate carrier
SLC	Solute carrier
Sp1	Specificity protein 1
VDR	Vitamin D receptor

Supplementary Information

The online version contains supplementary material available at https://doi.org/10.1186/s12987-024-00566-0.

Additional file 1. Additional Figures, Figures S1-S6..

Acknowledgements
The authors thank Dr. Jeffrey Henderson (Department of Pharmaceutical Sciences, University of Toronto, Canada) for his insight on immunocytochemical studies and Qing Rui Qu (Department of Pharmaceutical Sciences, University of Toronto, Canada) for his assistance on preliminary gene expression studies.

Author contributions
VS and RB participated in research design; VS and SA conducted experiments; RB contributed reagents or analytical tools; VS and RB performed data analysis; VS and RB wrote or contributed to the writing of the manuscript. All authors provided critical review of the manuscript and have given approval to the final version of the manuscript. All authors read and approved the final manuscript.

Funding
This work is supported by a Natural Sciences and Engineering Research Council of Canada (NSERC) operating grant (498383) awarded to Dr. Reina Bendayan. Vishal Sangha is a recipient of the Ontario Graduate Scholarship, Leslie Dan Faculty of Pharmacy Dean's Scholarship, and Dr. Heather Boon Award for Natural Health Products & Traditional Medicine Research.

Availability for data and materials
The datasets used and/or analysed during the current study are available from the corresponding author on reasonable request.

Declarations

Ethics approval and consent to participate
Not applicable.

Consent for publication
Not applicable.

Competing interests
The authors declare no competing interests.

Received: 16 April 2024 Accepted: 13 August 2024
Published online: 27 August 2024

References

1. Bailey LB, Rampersaud GC, Kauwell GPA. Folic acid supplements and fortification affect the risk for neural tube defects, vascular disease and cancer: evolving science. J Nutr. 2003;133(6):1961–8.
2. Alam C, Kondo M, O'Connor DL, Bendayan R. Clinical implications of folate transport in the central nervous system. Trends Pharmacol Sci. 2020;41(5):349–61. https://doi.org/10.1016/j.tips.2020.02.004.
3. Scaranti M, Cojocaru E, Banerjee S, Banerji U. Exploiting the folate receptor α in oncology. Nat Rev Clin Oncol. 2020;17:349–59.
4. Zhao R, Goldman ID. Folate and thiamine transporters mediated by facilitative carriers (SLC19A1-3 and SLC46A1) and folate receptors. Mol Aspects Med. 2013;34(2–3):373–85. https://doi.org/10.1016/j.mam.2012.07.006.
5. Dang Y, Zhou D, Du X, Zhao H, Lee CH, Yang J, et al. Molecular mechanism of substrate recognition by folate transporter SLC19A1. Cell Discov. 2022;8(1):141.
6. Zhao R, Aluri S, Goldman ID. The proton-coupled folate transporter (PCFT-SLC46A1) and the syndrome of systemic and cerebral folate deficiency of infancy: hereditary folate malabsorption. Mol Aspects Med. 2017;53:57–72.
7. Matherly LH, Schneider M, Gangjee A, Hou Z. Biology and therapeutic applications of the proton-coupled folate transporter. Expert Opin Drug Metab Toxicol. 2022;18:695–706.
8. Grapp M, Wrede A, Schweizer M, Hüwel S, Galla HJ, Snaidero N, et al. Choroid plexus transcytosis and exosome shuttling deliver folate into brain parenchyma. Nat Commun. 2013;4:2123.
9. Alam C, Hoque MT, Finnell RH, Goldman ID, Bendayan R. Regulation of reduced folate carrier (RFC) by vitamin D receptor at the blood-brain barrier. Mol Pharm. 2017;14(11):3848–58.
10. Alam C, Aufreiter S, Georgiou CJ, Hoque MT, Finnell RH, O'Connor DL, et al. Upregulation of reduced folate carrier by Vitamin D enhances brain folate uptake in mice lacking folate receptor alpha. Proc Natl Acad Sci USA. 2019;116(35):17531–40.
11. Alam C, Hoque MT, Sangha V, Bendayan R. Nuclear respiratory factor 1 (NRF-1) upregulates the expression and function of reduced folate carrier (RFC) at the blood-brain barrier. FASEB J. 2020;34(8):10516–30.
12. Zhao R, Min SH, Wang Y, Campanella E, Low PS, Goldman ID. A role for the proton-coupled folate transporter (PCFT-SLC46A1) in folate receptor-mediated endocytosis. J Biol Chem. 2009;284(7):4267–74.
13. Pope S, Artuch R, Heales S, Rahman S. Cerebral folate deficiency: analytical tests and differential diagnosis. J Inherit Metab Dis. 2019;42(4):655–72.
14. Ramaekers VT, Quadros EV. Cerebral folate deficiency syndrome: early diagnosis, intervention and treatment strategies. Nutrients. 2022;14:3096.
15. Goldman ID. FOLR1-related cerebral folate transport deficiency. In: Adam MP, Feldman J, Mirzaa GM, et al., editors. GeneReviews®. Seattle: University of Washington; 1993–2024.
16. Bobrowski-Khoury N, Ramaekers VT, Sequeira JM, Quadros EV. Folate receptor alpha autoantibodies in autism spectrum disorders: diagnosis, treatment and prevention. J Pers Med. 2021;11:710.
17. Erlacher M, Grünert SC, Cseh A, Steinfeld R, Salzer U, Lausch E, et al. Reversible pancytopenia and immunodeficiency in a patient with hereditary folate malabsorption. Pediatr Blood Cancer. 2015;62(6):1091–4. https://doi.org/10.1002/pbc.25364.

18. Sangha V, Aboulhassane S, Qu QR, Bendayan R. Protective effects of pyrroloquinoline quinone in brain folate deficiency. Fluids Barriers CNS. 2023;20(1):84.
19. Wu Z, Puigserver P, Andersson U, Zhang C, Adelmant G, Mootha V, et al. Mechanisms controlling mitochondrial biogenesis and respiration through the thermogenic coactivator PGC-1. Cell. 1999;98(1):115–24.
20. Chowanadisai W, Bauerly KA, Tchaparian E, Wong A, Cortopassi GA, Rucker RB. Pyrroloquinoline quinone stimulates mitochondrial biogenesis through cAMP response element-binding protein phosphorylation and increased PGC-1α expression. J Biol Chem. 2010;285(1):142–52. https://doi.org/10.1074/jbc.M109.030130.
21. Uchida Y, Goto R, Usui T, Tachikawa M, Terasaki T. Blood-arachnoid barrier as a dynamic physiological and pharmacological interface between cerebrospinal fluid and blood. In: de Lange ECM, Hammarlund-Udenaes M, Thorne RG, editors. Drug delivery to the brain: physiological concepts, methodologies and approaches. Cham: Springer International Publishing; 2022. p. 93–121. https://doi.org/10.1007/978-3-030-88773-5_4.
22. Sangha V, Williams EI, Ronaldson PT, Bendayan R. Drug transport in the brain. In: Drug transporters. 2022a. p. 283–317. https://doi.org/10.1002/9781119739883.ch14
23. Nabeshima S, Reese TS, Landis DMD, Brightman MW. Junctions in the meninges and marginal glia. J Comp Neurol. 1975;164(2):127–69.
24. Vandenabeele F, Creemers J, Lambrichts I. Ultrastructure of the human spinal arachnoid mater and dura mater. J Anat. 1996;189:417.
25. Thorne RG. Primer on central nervous system structure/function and the vasculature, ventricular system, and fluids of the brain. In: Hammarlund-Udenaes M, de Lange E, Thorne RG (eds) Drug delivery to the brain. Physiological concepts, methodologies and approaches. Springer, New York, 2014; 685–707
26. Gomez-Zepeda D, Taghi M, Scherrmann JM, Decleves X, Menet MC. ABC transporters at the blood–brain interfaces, their study models, and drug delivery implications in gliomas. Pharmaceutics. 2020;12(1):20.
27. Sangha V, Hoque MT, Henderson JT, Bendayan R. Novel localization of folate transport systems in the murine central nervous system. Fluids Barriers CNS. 2022;19(1):1–13. https://doi.org/10.1186/s12987-022-00391-3.
28. Yasuda K, Cline C, Vogel P, Onciu M, Fatima S, Sorrentino BP, et al. Drug transporters on arachnoid barrier cells contribute to the blood-cerebrospinal fluid barrier. Drug Metab Dispos. 2013;41(4):923–31.
29. Gilmore JC, Hoque MdT, Dai W, Mohan H, Dunk C, Serghides L, et al. Interaction between dolutegravir and folate transporters and receptor in human and rodent placenta. EBioMedicine. 2022;75:103771. https://doi.org/10.1016/j.ebiom.2021.103771.
30. Ronaldson PT, Bendayan R. HIV-1 viral envelope glycoprotein gp120 triggers an inflammatory response in cultured rat astrocytes and regulates the functional expression of P-glycoprotein. Mol Pharmacol. 2006;70(3):1087.
31. Schachenmayr W, Friede RL. The origin of subdural neomembranes. I. Fine structure of the dura-arachnoid interface in man. Am J Pathol. 1978;92(1):53–68.
32. Assaraf YG. The role of multidrug resistance efflux transporters in antifolate resistance and folate homeostasis. Drug Resist Updates. 2006;9(4–5):227–46.
33. Hinken M, Halwachs S, Kneuer C, Honscha W. Subcellular localization and distribution of the reduced folate carrier in normal rat tissues. Eur J Histochem. 2011;55(1):11–8.
34. Tetef ML, Margolin KA, Doroshow JH, Akman S, Leong LA, Morgan RJ, et al. Pharmacokinetics and toxicity of high-dose intravenous methotrexate in the treatment of leptomeningeal carcinomatosis. Cancer Chemother Pharmacol. 2000;46(1):19–26. https://doi.org/10.1007/s002800000118.
35. Wang X, Cabrera RM, Li Y, Miller DS, Finnell RH. Functional regulation of P-glycoprotein at the blood-brain barrier in proton-coupled folate transporter (PCFT) mutant mice. FASEB J. 2013;27(3):1167–75.
36. Huang C, Hoque T, Bendayan R. Antiretroviral drugs efavirenz, dolutegravir and bictegravir dysregulate blood-brain barrier integrity and function. Front Pharmacol. 2023;14:1118580.
37. Ueno M, Chiba Y, Murakami R, Miyai Y, Matsumoto K, Wakamatsu K, et al. Transporters, ion channels, and junctional proteins in choroid plexus epithelial cells. Biomedicines. 2024;12(4):708.
38. Chou YF, Yu CC, Huang RFS. Changes in mitochondrial DNA deletion, content, and biogenesis in folate-deficient tissues of young rats depend on mitochondrial folate and oxidative DNA injuries. J Nutr. 2007;137(9):2036–42.
39. Thakur S, Rahat B, Hamid A, Najar RA, Kaur J. Identification of regulatory mechanisms of intestinal folate transport in condition of folate deficiency. J Nutr Biochem. 2015;26(10):1084–94. https://doi.org/10.1016/j.jnutbio.2015.05.002.
40. Liu M, Ge Y, Cabelof DC, Aboukameel A, Heydari AR, Mohammad R, et al. Structure and regulation of the murine reduced folate carrier gene: identification of four noncoding exons and promoters and regulation by dietary folates. J Biol Chem. 2005;280(7):5588–97.
41. Kitamura Y, Hirouchi M, Kusuhara H, Schuetz JD, Sugiyama Y. Increasing systemic exposure of methotrexate by active efflux mediated by multidrug resistance-associated protein 3 (Mrp3/Abcc3). J Pharmacol Exp Ther. 2008;327(2):465.
42. Kitamura Y, Kusuhara H, Sugiyama Y. Basolateral efflux mediated by multidrug resistance-associated protein 3 (Mrp3/Abcc3) facilitates intestinal absorption of folates in mouse. Pharm Res. 2010;27(4):665–72.
43. Chern CL, Huang RFS, Chen YH, Cheng JT, Liu TZ. Folate deficiency-induced oxidative stress and apoptosis are mediated via homocysteine-dependent overproduction of hydrogen peroxide and enhanced activation of NF-κB in human Hep G2 cells. Biomed Pharmacother. 2001;55(8):434–42.
44. Wang F, Ji S, Wang M, Liu L, Li Q, Jiang F, et al. HMGB1 promoted P-glycoprotein at the blood-brain barrier in MCAO rats via TLR4/NF-κB signaling pathway. Eur J Pharmacol. 2020;880:173189.
45. Obaid M, Udden SMN, Alluri P, Mandal SS. LncRNA HOTAIR regulates glucose transporter Glut1 expression and glucose uptake in macrophages during inflammation. Sci Rep. 2021;11(1):232.
46. Gurler G, Belder N, Beker MC, Sever-Bahcekapili M, Uruk G, Kilic E, et al. Reduced folate carrier 1 is present in retinal microvessels and crucial for the inner blood retinal barrier integrity. Fluids Barriers CNS. 2023;20(1):1–19
47. Huang C, Fan Z, Han D, Johnston LJ, Ma X, Wang F. Pyrroloquinoline quinone regulates the redox status in vitro and in vivo of weaned pigs via the Nrf2/HO-1 pathway. J Anim Sci Biotechnol. 2021;12(1):1–17.

Publisher's Note